

DOI: 10.1002/chem.201204275

K...F/O Interactions Bridge Copper(I) Fluorinated Alkoxide Complexes and Facilitate Dioxygen Activation

June S. Lum,^[a] Laleh Tahsini,^[a] James A. Golen,^[b, c] Curtis Moore,^[c]
Arnold L. Rheingold,^[c] and Linda H. Doerr*^[a]

Abstract: Seven E[Cu(OR)₂] copper(I) complexes (E = K⁺, {K(18C6)}⁺ (18C6 = [18]crown-6), or Ph₄P⁺; R = C₄F₉, CPhMe^F₂, and CMeMe^F₂) have been prepared and their reactivity with O₂ studied. The K[Cu(OR)₂] species react with O₂ in a copper-concentration-dependent manner such that 2:1 and 3:1 Cu/O₂ adducts are observed manometrically at -78 °C. Analogous reactivity with O₂ is not observed with the {K(18C6)}⁺ or Ph₄P⁺ derivatives.

Solution conductivity data demonstrate that these K[Cu(OR)₂] complexes do not behave as 1:1 electrolytes in solution. The K⁺ ions induce aggregation of multiple [Cu(OR)₂]⁻ units through K...F/O interactions and thereby effect irreversible O₂ reduction by multiple

Cu centers. Bond valence analyses for the potassium cations confirm the dominance of the fluorine interactions in the coordination spheres of K⁺ ions. Intramolecular hydroxylation of ligand aryl and alkyl C-H bonds is observed. Nucleophilic reactivity with CO₂ is observed for the oxygenated Cu complexes and a Cu^{II} carbonate has been isolated and characterized.

Keywords: C-H activation • copper • dioxygen reactivity • fluorinated ligands • K...F/O interaction

Introduction

The dioxygen reactivity of Cu^I complexes and the oxidative properties of the resulting Cu/O₂ species have gained widespread attention in small-molecule catalysis^[1] and biological^[2] systems. Distinct oxygenated products are produced from one-, two-, and four-electron reduction of dioxygen by Cu^I complexes, leading to superoxide, peroxide, and oxide species. The majority of Cu^I complexes used to generate well-characterized oxygenated species in biomimetic studies contain aromatic nitrogen-donor ligands (pyrazole, pyridine, and imidazole) and ligands with aliphatic amine groups.^[3] Herein, we report that O₂ reduction and subsequent C-H hydroxylation chemistry can be achieved with Cu^I bound to oxygen-donor, fluorinated alkoxide ligands as well. Heterobimetallic Ba^{II}-Cu^I,^[4] Ba^{II}-Cu^{II},^[5] and Al^{III}-Cu^{II}^[6] complexes with partially fluorinated alkoxides and hetero-^[7] and homo-

metallic^[8] Cu^{II} complexes with partially fluorinated and non-fluorinated alkoxides have also been previously synthesized. Although numerous syntheses exist for Cu^I alkoxide complexes, prior to this report there had been only one report of their reactivity with O₂, in which non-fluorinated alkoxide {Cu(OR)}_n species reacted with O₂ to give ligand-derived aldehydes or ketones in low yields.^[9]

Homoleptic complexes of 3d transition metals, including Fe^{II},^[10] Fe^{III},^[10b] Co^{II},^[10a,11] Ni^{II},^[12] and Cu^{II},^[11,13] have been prepared with completely fluorinated aryloxy and alkoxide ligands. These aryloxides and alkoxides are medium-field ligands, such as OH⁻ or F⁻, from UV/Vis spectroscopic^[10-13] and DFT^[10b] studies. Ligand fluorination also reduces bridging in metal complexes due to the diminished basicity of the O donor atom, resulting in the formation of discrete monomeric species.^[10,11] Such fluorinated ligands should be ideal for stabilizing transition metals, even transiently, in high oxidation states for C-H activation studies in which intramolecular C-H activation is less likely or impossible. Extending our studies to Cu^I, we have synthesized a series of Cu^I alkoxide complexes with varying degrees of ligand fluorination, OC₄F₉, OCPHMe^F₂, and OCMeMe^F₂, and studied their O₂ reactivity. The extensive K⁺-ligand interactions observed are demonstrated to effect dioxygen reduction and subsequent C-H activation or CO₃²⁻ formation by assembling polynuclear {Cu_n} units in solution.

Results and Discussion

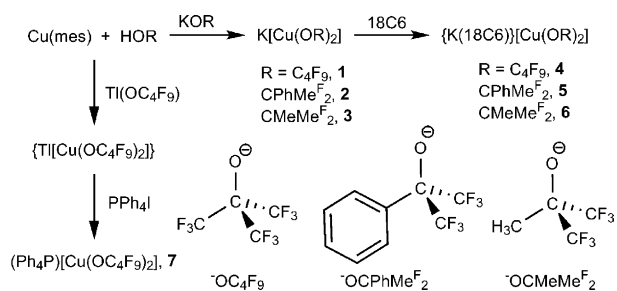
Syntheses: A modified alcoholysis route^[10a,11] was used to prepare the homoleptic Cu^I compounds (Scheme 1). The

[a] Dr. J. S. Lum, Dr. L. Tahsini, Prof. Dr. L. H. Doerr
Department of Chemistry, Boston University
590 Commonwealth Avenue, Boston, MA 02215 (USA)
Fax: (+1) 617-353-6466
E-mail: doerr@bu.edu

[b] Prof. Dr. J. A. Golen
Department of Chemistry and Biochemistry
University of Massachusetts, Dartmouth
285 Old Westport Road, North Dartmouth, MA 02747 (USA)

[c] Prof. Dr. J. A. Golen, Dr. C. Moore, Prof. Dr. A. L. Rheingold
Department of Chemistry and Biochemistry
University of California, San Diego
9500 Gilman Drive, La Jolla, CA 92093 (USA)

Supporting information for this article is available on the WWW under <http://dx.doi.org/10.1002/chem.201204275>.



Scheme 1. Syntheses of Cu^{I} fluorinated alkoxide complexes. 18C6 = [18]crown-6, mes = mesityl.

salt, KOC_4F_9 , has been reported previously.^[4,14] The potassium salts of the ligands $\text{KOCPhMe}_2^{\text{F}}$ and $\text{KOCMe}_2^{\text{F}}$ were synthesized from the reaction of HOR with KH. Three anionic Cu^{I} complexes were prepared by the reaction of $\{\text{Cu}(\text{mes})\}_n$ with HOR and the addition of one equivalent of KOR, resulting in $\text{K}[\text{Cu}(\text{OC}_4\text{F}_9)_2]$ (**1**), $\text{K}[\text{Cu}(\text{OCPhMe}_2^{\text{F}})_2]$ (**2**), and $\text{K}[\text{Cu}(\text{OCMe}_2^{\text{F}})_2]$ (**3**). The 18C6 complexes $\{\text{K}(18\text{C}6)\}[\text{Cu}(\text{OC}_4\text{F}_9)_2]$ (**4**), $\{\text{K}(18\text{C}6)\}[\text{Cu}(\text{OCPhMe}_2^{\text{F}})_2]$ (**5**), and $\{\text{K}(18\text{C}6)\}[\text{Cu}(\text{OCMe}_2^{\text{F}})_2]$ (**6**) were prepared for increased solubility with unexpected effects on reactivity (see below). $\text{Ti}(\text{OC}_4\text{F}_9)_2$ was used to prepare $\text{Ti}[\text{Cu}(\text{OC}_4\text{F}_9)_2]$ (in situ), leading to $(\text{Ph}_4\text{P})[\text{Cu}(\text{OC}_4\text{F}_9)_2]$ (**7**) by cation metathesis reaction. Complexes **4**, **5**, and **6** were soluble in both toluene and CH_2Cl_2 , whereas compound **7** was soluble only in CH_2Cl_2 .

Structural characterization: X-ray crystallographic data were obtained for $\text{KOCPhMe}_2^{\text{F}}$, $\text{KOCMe}_2^{\text{F}}$, $\text{Ti}(\text{OC}_4\text{F}_9)_2$, and complexes **1**, **2**, **4**, **6**, and **7**. For the three ligand salts, data collection parameters are given in Table S1 in the Supporting Information with selected metrical information in Table S2. Data collection parameters for the copper alkoxide complexes are given in Table S3 in the Supporting Information with selected metrical information in Table S4.

The MOR salts of the ligands have cubane structures with the general formula $[\text{M}(\text{OR})_4]$, similar to that of KOC_4F_9 ,^[10a,12] and are shown in Figures S1–S3 in the Supporting Information. Similar tetrameric fluorinated alkoxide structures of $[\text{Li}(\text{OC}_4\text{F}_9)_4]^{[15]}$ and $[\text{Na}(\text{OC}_4\text{F}_9)_4]^{[16]}$ have been reported previously.

All of the anionic $[\text{Cu}(\text{OR})_2]^-$ compounds have effectively linear two-coordinate Cu^{I} centers. Complex **1** has $\text{Cu}-\text{O}$ bond lengths of 1.852(2) and 1.832(2) Å and the K^+ cation has an $\{\text{O}_3\text{F}_7\}$ coordination environment. Seven $\text{K}\cdots\text{F}$ (average 2.96(11) Å) and three $\text{K}\cdots\text{O}$ (average 2.76(10) Å) interactions link the $[\text{Cu}(\text{OC}_4\text{F}_9)_2]^-$ anions in the solid state, as shown in Figures 1 and 2. Related $\text{Na}\cdots\text{F}$ interactions have been described for $\text{Na}_2\{\text{Cu}[\text{OCH}(\text{Me}^{\text{F}})_2]_2\}^{[17]}$ and the $[\text{NaOR}]_4$ cubanes ($\text{R} = \text{CMe}_2\text{Me}^{\text{F}}$ and C_4F_9).^[16]

The $\text{Cu}1-\text{O}1$ and $\text{Cu}1-\text{O}2$ distances in **2** of 1.8666(18) and 1.8665(18) Å, respectively, are slightly longer than those in **1**, and an almost linear $\text{O}1-\text{Cu}-\text{O}2$ angle of 176.14(8)° is observed. Bridging $\text{K}\cdots\text{F}/\text{O}$ interactions are also present in **2**, such that each K^+ cation has an $\{\text{O}_2\text{F}_6\}$ coordination

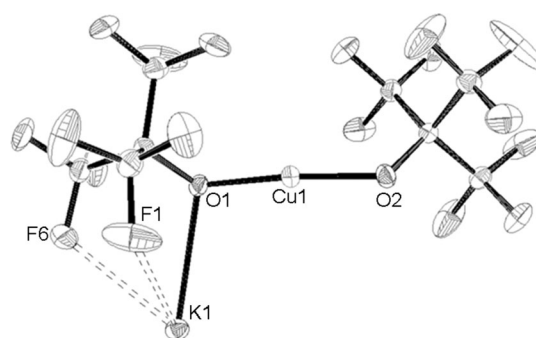


Figure 1. ORTEP diagram of complex **1**, showing two $\text{K}\cdots\text{F}$ interactions in the solid state per molecule (dotted lines to F ellipsoids). Ellipsoids are shown at the 50% probability level.

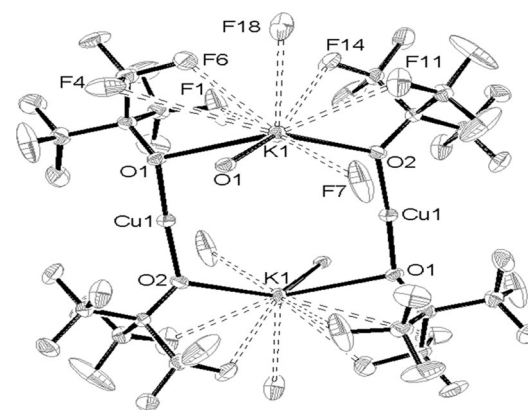


Figure 2. ORTEP diagram of complex **1**, showing that multiple $\text{K}\cdots\text{F}$ interactions bridge two $[\text{Cu}(\text{OC}_4\text{F}_9)_2]^-$ anions. Ellipsoids are shown at the 50% probability level.

sphere (Figure 3). In addition, **2** exhibits two crystallographically independent solid-state cuprophilic interactions, with $\text{Cu}\cdots\text{Cu}$ distances of 2.5566(6) and 2.5558(6) Å (sum of two Cu atom van der Waals radii is 2.80 Å). Metallophilic interactions between Cu centers were first observed in $[\text{Cu}(\text{CH}_2\text{SiMe}_3)_4]^{[18]}$ and have subsequently been reviewed.^[19] As

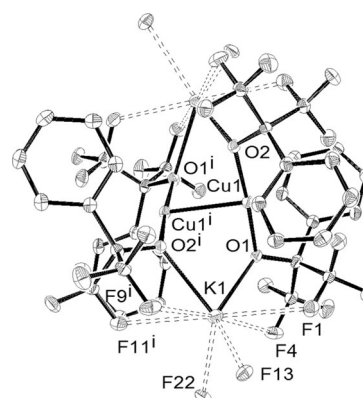


Figure 3. ORTEP diagram of one crystallographically independent unit of **2**. One $\text{Cu}\cdots\text{Cu}$ cuprophilic interaction is shown (2.5558(6) Å) and dotted lines indicate bridging $\text{K}\cdots\text{F}$ interactions. Hydrogen atoms are removed for clarity and ellipsoids are shown at the 50% probability level.

with the better-studied aurophilic compounds, cuprophilicity is most often observed between d^{10} centers with linear coordination. In comparison to other cuprophilic interactions reported in the literature,^[19] those $\text{Cu}\cdots\text{Cu}$ interactions in **2** are short; this phenomenon is due to the bridging K^+ ions shown in Figure 3.

In **4** and **6** (Figures S4 and S5 in the Supporting Information), the number of $\text{K}\cdots\text{F}/\text{O}$ alkoxide contacts decreases when K^+ is encapsulated by 18C6. For **4**, the Cu1-O7 and Cu1-O8 distances are 1.865(6) and 1.861(7) Å, respectively, both are noticeably longer than those in **1**, and the O7-Cu-O8 angle is 172.0(3)°. In contrast, in **6**, the Cu1-O7 bond length is 1.8152(19) Å and the Cu1-O8 length is 1.805(2) Å, both are much shorter than those in **2**, with a linear O7-Cu-O8 angle of 172.34(9)°. Complex **7** (Figure S6 in the Supporting Information), with the Ph_4P^+ cation, has Cu-O bond lengths of 1.8297(17) and 1.8289(17) Å, which are slightly contracted compared with the same Cu-O bond lengths in **1**. A comparison of the new Cu^{I} alkoxide structures with several from past work is presented in Table S5 in the Supporting Information.

Bond valence analysis: Bond valence^[20] is a useful concept for analyzing bond distance data obtained from single-crystal X-ray diffraction studies and quantifying the relative contributions to the coordination sphere of a metal ion. The bond valence value, s , provides a quantitative measure^[21] of how much the secondary $\text{K}\cdots\text{F}/\text{O}$ interactions contribute to the coordination sphere of each K^+ cation. The bond valences (s) were obtained by using the appropriate bond valence parameters^[20,21] and Equation (1)

$$s = e^{\frac{(R_{\text{K-F}} - d_{\text{K-F/O}})}{B}} \quad (1)$$

in which $R_{\text{K-F}} = 1.992$, $R_{\text{K-O}} = 2.132$, $B = 0.37$, and $d_{\text{K-F/O}}$ are the $\text{K}\cdots\text{F}$ or K-O distances obtained from crystallographic data. The sums of the bond valence values ($\Sigma(s)$) for each K^+ ion in the Cu^{I} alkoxides have been calculated (Table 1) and approach unity, as expected, for a monovalent cation. The same analysis for $\text{KOCPhMe}^{\text{F}_2}$ and $\text{KOCMeMe}^{\text{F}_2}$ gives similar results and is presented in Table S6 in the Supporting Information.

The potassium cation in **1** has a $\{\text{O}_3\text{F}_7\}$ coordination sphere with 49% of the valence contributed by $\text{K}\cdots\text{F}$ contacts alone, and the remaining coordination sphere filled out

by the K-O interactions to the alkoxide ligands. These seven $\text{K}\cdots\text{F}$ distances in **1** range from 2.810(2) to 3.086(3) Å, in bridging both within and between the anions (Figure 2).

A similar contribution of $\text{K}\cdots\text{F}$ contacts was quantified for the three crystallographically unique potassium cations in **2**. Each K^+ cation has a coordination sphere of $\{\text{O}_2\text{F}_6\}$ and an average of 48% is donated to the total bond valence by $\text{K}\cdots\text{F}$ interactions. The average $\text{K}\cdots\text{F}$ distances are longer in **2** than those in **1**, and overall smaller values of s were calculated for those lengthier $\text{K}\cdots\text{F}$ contacts.

The bond valence analysis for the encapsulated K^+ cations in **4** and **6** showed that the six K-O bonds from 18C6 dominated the K^+ environment, with $\{\text{O}_7\text{F}_1\}$ coordination for both, and the $\text{K}\cdots\text{F}$ contributions are less than 7% in each case. Clearly, ensnaring the K^+ cation by the cyclic crown ether molecule in **4** and **6** produces discrete $[\text{Cu}(\text{OR})_2]^-$ anions with fewer bridging contacts, impacting the solubility and solution-state conductivity behavior of the complexes.

Solution-state conductivity: The solution conductivities of the $\{\text{ECu}(\text{OR})_2\}$ complexes, in which $\text{E} = \text{K}^+$, $[\text{K}(18\text{C6})]^+$, or Ph_4P^+ , were measured in THF and CH_2Cl_2 to determine their degree of electrolyte behavior. Solution-state conductivity data were acquired for solutions of **1**, **2**, **3**, and **7** in THF and for solutions of **4**, **5**, **6**, and **7** in CH_2Cl_2 . The 1:1 electrolyte TBAPF_6 ($\text{TBAPF}_6 = n\text{Bu}_4\text{NPF}_6$ in THF or CH_2Cl_2) and non-electrolyte $[\text{FeCp}_2]$ (in THF; Cp = cyclopentadiene) were used as reference solutions. The Onsager plots^[22] for complexes **1**, **4** and **7** are shown in Figure 4; those for **2** and **5** are in Figure S7 in the Supporting Infor-

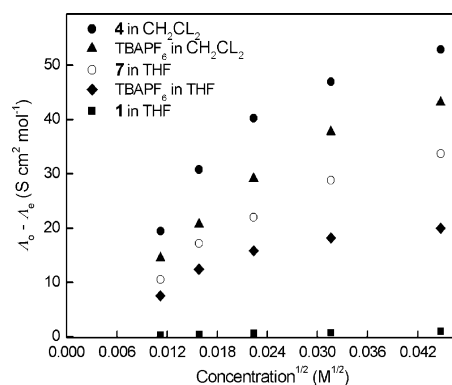


Figure 4. Solution conductivity studies of $[\text{Cu}(\text{OC}_4\text{F}_9)_2]^-$ derivatives **1**, **4**, **7**, and TBAPF_6 in THF and CH_2Cl_2 .

Table 1. K^+ bond valence analysis for $\{\text{K}[\text{Cu}(\text{OR})_2]\}$ complexes.

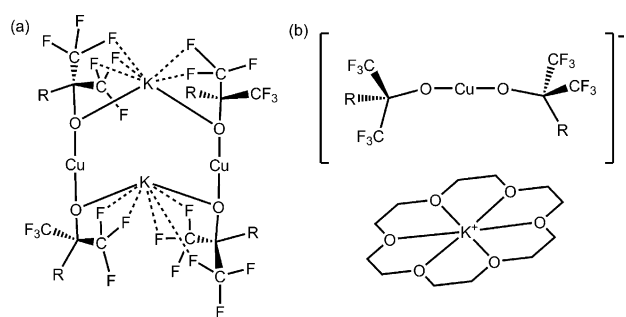
	K^+ coordination sphere	$\Sigma(s)^{[a]}$	$\Sigma(s) \text{K}\cdots\text{F} [\%]$	$\text{K}\cdots\text{F} [\text{Å}]$	$s(\text{K}\cdots\text{F})$
1	$\text{K1 O}_3\text{F}_7$	1.09	49	2.810(2)–3.086(3)	0.052–0.110
2	$\text{K1 O}_2\text{F}_6$	0.940	48	2.865(2)–3.174(2)	0.041–0.094
	$\text{K2 O}_2\text{F}_6$	0.925	47	2.884(2)–3.179(2)	0.040–0.090
	$\text{K3 O}_2\text{F}_6$	0.953	48	2.869(2)–3.154(2)	0.043–0.093
4	$\text{K1 O}_7\text{F}_1$	1.21	6.3	2.945(7)	0.076
	$\text{K1 O}_7\text{F}_1$	1.08	5.8	3.015(2)	0.063

[a] Calculated by using Equation (1), in which $R_{\text{K-F}} = 1.992$, $R_{\text{K-O}} = 2.132$, $B = 0.37$,^[20,21] and $d_{\text{K-F/O}}$ are the crystallographically determined $\text{K}\cdots\text{F}$ or K-O distances.

ation, and those for **3** and **6** in Figure S8 along with the control 1:1 electrolyte and non-electrolyte measurements. The solvent THF was hypothesized to disrupt any $\text{K}\cdots\text{F}/\text{O}$ interactions due to the weak basicity of the fluorinated alkoxides ($\text{p}K_a(\text{HOC}_4\text{F}_9) = 5.4$ and $\text{p}K_a(\text{HOCMeMe}^{\text{F}_2}) = 9.6$),^[23] and therefore, yield 1:1 electrolytes, regardless of the encapsulation of K^+ .

Interestingly, complex **1** did not exhibit the conductivity of a 1:1 electrolyte. Complexes **1**, **2**, and **3** all showed decreased conductivities relative to their corresponding $\{K(18C6)\}^+$ derivatives (**4**, **5**, and **6**), which did behave as 1:1 electrolytes. The increased fluorination and $K\cdots F$ interactions are proposed to account for the decreased conductivity of **1** in THF versus **2** or **3**. The $\{K(18C6)\}^+$ species **4–6** and Ph_4P^+ **7** displayed increased conductivity in THF and CH_2Cl_2 , consistent with a low degree of ion pairing in solution.

The pattern of the conductivity studies matches the bimodal groupings in the bond valence analysis and strongly suggests that the observed bridging solid-state $K\cdots F/O$ interactions are maintained in solution for complexes **1**, **2** and **3**, which therefore behave as multinuclear $\{K[Cu(OCR(CF_3)_2)_2]\}_n$ units in solution (Scheme 2) and have less ionic



Scheme 2. a) Drawing of a proposed $\{K[Cu(OCR(CF_3)_2)_2]\}_2$ aggregate in solution with $K\cdots F/O$ interactions bringing two Cu^I centers. b) Discrete anionic $[Cu\{OCR(CF_3)_2\}_2]^-$ and cationic $\{K(18C6)\}^+$ units responsible for 1:1 electrolyte behavior in solution.

character than compounds **4–6** and **7**. In another study, a trinuclear Cu^I species, $\{K(18C6) K_2[Cu(OCPhMeF_2)_2]\}_3$,^[24] with three linear $[Cu(OCPhMeF_2)_2]^-$ anions held together by two unencapsulated K^+ cations has been characterized crystallographically. Extensive bridging $K\cdots F/O$ interactions between the $[Cu(OR)_2]^-$ groups and the non-encapsulated K^+ cations assemble a trinuclear Cu_3 core.^[24]

O₂ reaction stoichiometry: Exposure of solutions of **1**, **2**, and **3** in THF to O_2 at $-78^\circ C$ resulted in the rapid generation of intensely colored species, the Cu/O_2 stoichiometries of which were determined manometrically.^[25] Details of the error analysis are given in Table S7 in the Supporting Information. The O_2 uptake of these solutions at varying Cu concentrations is shown in Figure 5. Regardless of the $[Cu^I]$, the O_2 uptake of **1** was observed to have a 3:1 Cu/O_2 ratio. In contrast, a 2:1 Cu/O_2 stoichiometry for solutions with $[Cu^I]$ less than 2 mM and a 3:1 Cu/O_2 ratio for $[Cu^I]$ greater than 3 mM was observed for complexes **2** and **3**. A non-integral Cu/O_2 ratio was obtained at Cu concentrations between 2 and 3 mM, which increased linearly between the regions of integral ratios. Di- $\{Cu_2-O_2\}$ and trinuclear $\{Cu_3-O_2\}$ intermediates^[3,26] have previously been observed with N-donor li-

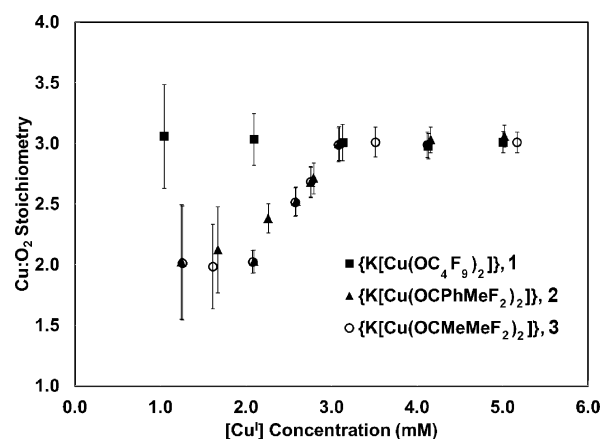


Figure 5. Cu/O_2 stoichiometry determined by manometry for complexes **1–3** in THF at $-78^\circ C$.

gands, but the observation of both with the same ligand is extremely rare.^[27]

UV/Vis spectroscopy of $\{Cu_n-O_2\}$ species: Exposing colorless to pale-yellow solutions of complexes **1–3** in THF to dry O_2 at $-80^\circ C$ caused a relatively rapid color change to purple (**1**), dark blue (**2**), and dark red-brown (**3**). As indicated in Table 2, all Cu^I complexes exhibit a single strong

Table 2. UV/Vis spectral data for compounds **1–3**.

Compound	Cu^I complex ^[a]	Cu_n-O_2 adduct ^[a,b]		
1	240 (1790)	307 (nd) ^[c]	520 (448)	602 (406)
2	234 (4240)	315 (nd) ^[d]	496 (323)	590 (393)
		320 (nd) ^[e]	644 (104)	
3	236 (3000)	320 (nd) ^[d]	500 (858)	720 (170)
		320 (nd) ^[e]	511 (218)	673 (96)

[a] Absorption maxima (λ_{max}) are given in nanometers. Extinction coefficients are based on the Cu_n-O_2 species and are given in parentheses ($M^{-1}cm^{-1}$). [b] Solutions were oxygenated in THF at $-80^\circ C$. [c] Due to deviation from Beer's law, extinction coefficients could not be determined. [d] Observed in a 6.0 mM oxygenated solution of Cu^I . [e] Observed in a 2.0 mM oxygenated solution of Cu^I .

absorption band in the UV region, which is likely to be an O–Cu ligand-to-metal charge-transfer (LMCT) band. After exposure to O_2 , intense and multiple absorptions in the 300–350 nm region develop, but related molar absorptivity values could not be determined due to deviation from Beer's law. Other distinct absorbances for **1** occur at 520 ($\epsilon = 448$) and 602 nm ($406 M^{-1}cm^{-1}$) at all Cu concentrations studied, as shown in Figure 6a and Figure S9 in the Supporting Information, whereas oxygenated solutions of **2** revealed different chromophores, depending on the amount of Cu^I complex (Figure 6b). Introduction of O_2 into solutions of **2** with less than 2 mM Cu^I produces a species with a relatively weak absorption at 644 nm ($\epsilon = 104 M^{-1}cm^{-1}$). Oxygenation of **2** with greater than 3.0 mM Cu^I , however, generates a species with two visible absorptions at 496 ($\epsilon = 295 M^{-1}cm^{-1}$) and 590 nm ($\epsilon = 330 M^{-1}cm^{-1}$).

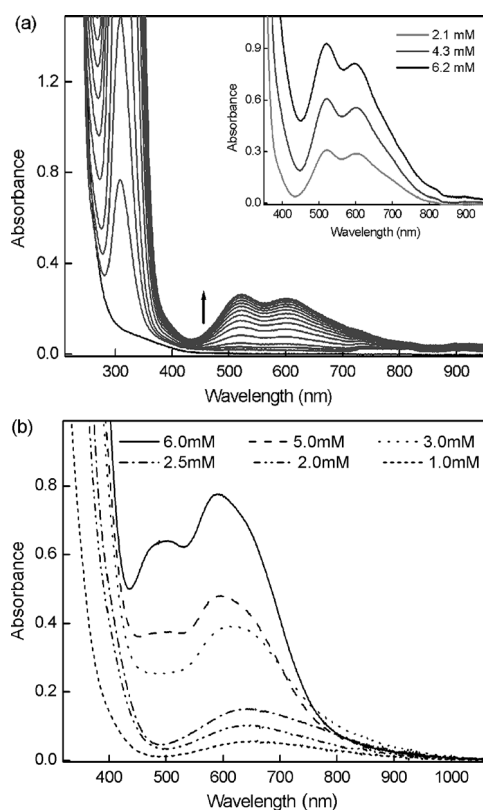


Figure 6. a) UV/Vis spectral changes observed upon the introduction of O_2 into a solution of **1** (2.1 mM) in THF at $-80^\circ C$. The inset shows a close up of the visible region of the generated O_2 adduct in different concentrations of **1**. b) UV/Vis spectra of generated chromophores in different concentrations of oxygenated solutions of **2** in THF at $-80^\circ C$.

Reaction of **3** with O_2 produces different chromophores for low and high concentrations of Cu^I , specifically affected by the concentration of O_2 in solution. When oxygen diffuses slowly through the headspace into a solution of **3** with 6 mM Cu^I , a broad band at 720 nm ($203\text{ M}^{-1}\text{ cm}^{-1}$) develops along with an intense broad absorption at about 500 nm covered by charge-transfer features at 300–450 nm (Figure 7a). The copper–oxygen adduct produced, likely $\{Cu_3-O_2\}$, is quite stable once fully formed, as indicated by the time profile of the oxygenation reaction (inset of Figure 7a) at 495 nm. The initial incomplete formation of the same chromophore was observed in **3** with 2 mM Cu^I (Figure 7b), however, it converts into a new species, likely $\{Cu_2-O_2\}$, with absorption bands at 511 and 700 nm shortly after formation (inset of Figure 7b).

The O_2 -reduction product of **3** is not only controlled by the Cu concentration, but also by the rate of O_2 diffusion into the solution. Generation of the $\{Cu_3-O_2\}$ adduct is favored at high Cu^I concentration under slow diffusion of O_2 ; these are the manometry experimental conditions. In contrast, fast/enforced O_2 introduction into the solution by bubbling leads to the $\{Cu_2-O_2\}$ species independent of Cu^I concentration. Scheme 3 shows how the generation of oxygenated species from **3** depends on the O_2 introduction method. Letting O_2 bubble through a 6 mM solution of **3** at $-80^\circ C$

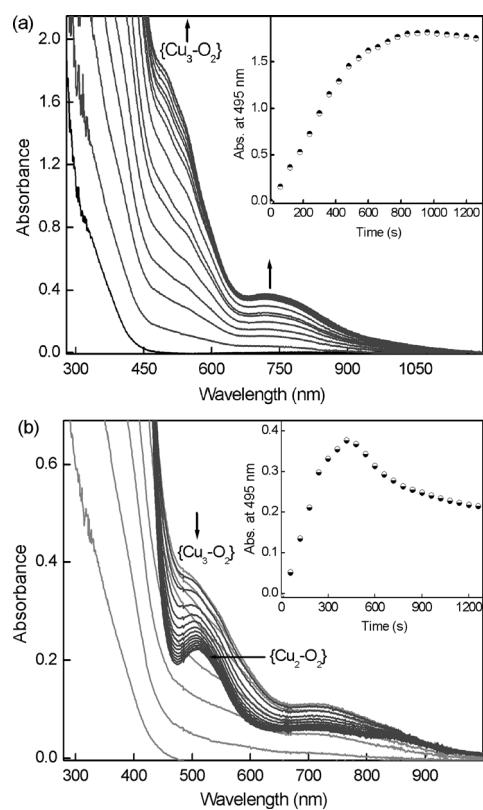
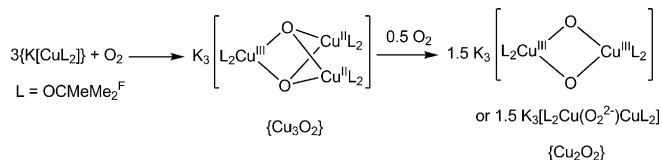


Figure 7. UV/Vis spectral changes observed upon the introduction of O_2 into a 6.0 (a) and 2.0 mM (b) solution of **3** in THF at $-80^\circ C$. The insets show the time profile of the absorbance at 495 nm due to $\{Cu_n-O_2\}$ species.



Scheme 3. The O_2 -concentration-dependent formation of $\{Cu_n-O_2\}$ species from **3**.

produced $\{Cu_2-O_2\}$ with an intense absorption at 511 nm and a broad band at 700 nm (Figure S9 in the Supporting Information). These spectral features are quite different from those observed in slow diffusion of O_2 into a solution of Cu^I (Figure 7). Interestingly, the $\{Cu_3-O_2\}$ adduct formed by slow diffusion of O_2 can be converted into the $\{Cu_2-O_2\}$ produced from O_2 bubbling through the solution (Figure S9 in the Supporting Information).

Chromophore formation for oxygenated solutions of **1**, **2**, or **3** is irreversible under vacuum or argon purge, but stability is maintained at $-80^\circ C$ for more than an hour in each case. Reactive complexes decompose quickly into green-brown solutions upon warming to room temperature, again indicative of irreversible O_2 reduction. Attempts to record resonance Raman spectra were unsuccessful.

Surprisingly, no chromophores were generated upon the addition of O_2 to **4** in toluene, or to **7** in CH_2Cl_2 , at $-80^\circ C$. These compounds with 1:1 electrolyte character were also

unreactive with O₂ in THF at –80 °C. Only upon warming to room temperature was oxidation evident through the slow evolution of the green color. The reactivity of the Cu^I alkoxides with O₂ is thus more facile in the presence of more K...F/O interactions. The di- or trinuclear aggregates of **1**, **2**, and **3** indicated by O₂ uptake measurements could provide up to four or six reducing electrons, respectively, for the irreversible reduction of O₂. Without the assembly of a polynuclear {Cu_n} core, the reaction with O₂ does not occur at –80 °C.

C–H bond hydroxylation and ¹⁸O₂ studies: The reduction of O₂ by **1**, **2**, and **3** is not reversible at –80 °C, and warming the reaction mixtures to room temperature changes the color of oxidized solutions to green–brown. The vulnerable phenyl C–H bonds of **2** and methyl C–H bonds of **3** were activated by insertion of an “O” atom to form hydroxyl groups. ESI-MS analysis of the oxygenated product of **2** at room temperature revealed an ion peak at *m/z* 259, the mass and isotope distribution of which corresponds to [OC(C₆H₄OH)Me^F₂][–], with a hydroxylated phenyl ring of the ligand. *ortho*-Hydroxylation of the phenyl ring for complex **2** is proposed, based on the favorability of six-membered chelate ring formation, which yields the *ortho*-hydroxylated ligand as the product of the reaction. Similarly the oxygenated product of **3** at room temperature is the ligand with a hydroxylated methyl substituent, as indicated by a peak at *m/z* 197, corresponding to [OC(CH₂OH)Me^F₂][–]. The ESI-MS data for the oxygenated solution of complex **1** after warming show only the OC₄F₉[–] ligand.

When the oxidation reactions were carried out with isotopically labeled ¹⁸O₂, ESI-MS analysis revealed a new peak at *m/z* 261 for **2** along with that observed earlier at *m/z* 259, and a new peak at *m/z* 199 for **3** along with one for *m/z* 197. The observation of an increase in *m/z* by two units upon isotopic substitution confirms the source of the hydroxyl O atom as ¹⁸O₂ (Figure 8). Three higher concentrations of complexes (4, 5, and 6 mM) were studied in oxygenation reactions of **2** and **3**, and all three trials revealed incorporation of ¹⁸O.

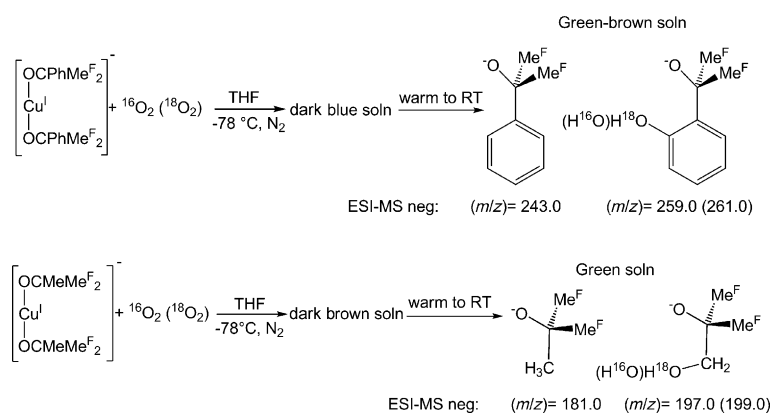


Figure 8. ¹⁶O₂ and ¹⁸O₂ reactivity of complexes **2** and **3**, showing hydroxylated C–H bonds of the ligands, with proposed regioselectivity for the phenyl ring resulting from **2** and O₂.

CO₂ reactivity: Some electrophilic character of the {Cu_nO₂}, *n* = 2 or 3, moieties was demonstrated in the phenyl hydroxylation of **2**. The nucleophilic character of the reduced oxygen species was demonstrated in their reaction with CO₂. It is unusual for these two disparate types of reactivity to be achieved with one ligand system. A Cu^I β-diketiminato system also generates a {Cu₃O₂} moiety and carbonate, but does not abstract H atoms.^[27d]

Reaction of O₂ with complexes **1**, **2**, and **3**, in Cu concentrations greater than 5 mM, was followed by the addition of CO₂ after removal of excess oxygen and resulted in the formation of green (**1**–CO₃ and **2**–CO₃) or blue (**3**–CO₃) powders. The recrystallization of **3**–CO₃ from dimethoxyethane (DME) afforded X-ray quality blue crystals of **3**–CO₃ and **8**, along with a green species that has not yet been identified.

The solid-state IR spectra for powders of **1**–CO₃, **2**–CO₃, and crystals of **8** are shown in Figure S10 and Table S8 in the Supporting Information, which lists the relevant IR-active stretches for carbonate vibrational modes and compares them with two other reported Cu^{II} carbonate species.^[28] The IR stretches are observed in the region of 1320–1550 cm^{–1}, consistent with a metal-bound CO₃^{2–} moiety.^[29] Similar IR stretches were reported for the Cu^{II} carbonate complexes {[Cu(pip)(H₂O)]₃–μ₃–CO₃}(ClO₄)₄^[28b] and [Cu₂(Me₂im)₆(CO₃)](PF₆)₂^[28a] (pip = 2-[2-(2-pyridyl)ethylimino-methyl]pyridine, Me₂im = 1,2-dimethylimidazole) and also for potassium carbonate.^[30] The other IR stretches are assigned as alkoxide-related vibration modes: 1199 (νC–F), 1175, 957 (νCu–OR), and 700 cm^{–1} (νC–F and νCu–OR).^[10a,30]

Compound **8** is a Cu^{II} alkoxide carbonate tetramer, the asymmetric unit of which is shown in Figure 9, along with the full tetramer in Figure 10. The four crystallographically identical Cu^{II} centers are bridged by CO₃^{2–} and K⁺ with the stoichiometry {[K₂(DME)_{1.5}][Cu(OCMeMe^F₂)₂(CO₃)]₄. Two alkoxide [–]OCMeMe^F₂ ligands are bound terminally to each Cu^{II} and bridged by a K⁺ cation, in which the Cu1–O4 and Cu1–O5 distances are 1.940(2) and 1.898(3) Å, respectively. The elongated bridging Cu–O_{alkoxide} distances are comparable to a similar Cu1–O8_{alkoxide} bond distance of 1.858(2) Å in **6** in which the bridging alkoxide distance is longer than the terminal alkoxide distance.^[24]

The two other coordination sites of each Cu^{II} center are filled by a bidentate carbonate, with Cu1–O2 and Cu1–O3 distances of 1.978(2) and 2.003(2) Å, respectively. The Cu1...O1 distance to the next asymmetric unit is nonbonding at 2.511(2) Å, effectively resulting in a four-coordinate geometry for Cu^{II}. The four-coordinate Cu^{II} center has a τ₄ value^[31] of 0.18, indicating a slight distortion from square-

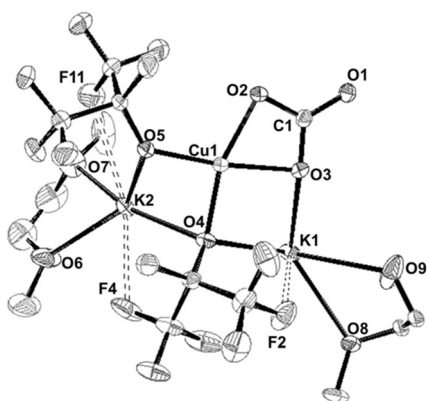


Figure 9. ORTEP drawing of one unit of tetrameric compound **8** with DME. Hydrogen atoms have been removed for clarity. Ellipsoids are drawn at the 50% probability level. Selected K...F interactions are depicted as dotted lines.

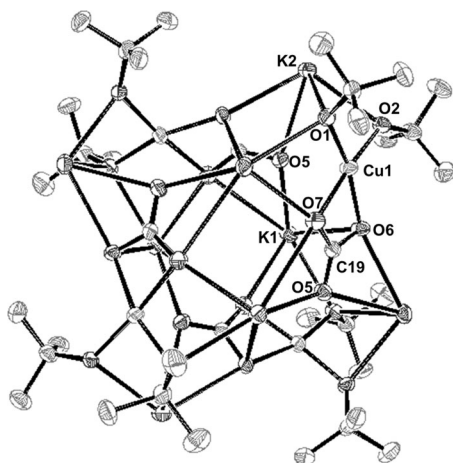


Figure 10. ORTEP drawing of **8** shown as a tetramer with DME molecules and fluorine atoms of ligand removed for clarity. Relevant atoms of a single monomeric unit are labeled. Ellipsoids are drawn at the 50% probability level.

planar geometry. The small bite-angle O2–Cu1–O3 of 66.8(1)° subtends the four-membered chelate ring and the bidentate binding mode of the CO₃²⁻ group with a O2–C1–O3 bond angle of 114.5(3)°.

The CF₃ groups of **8** also engage in K...F interactions like those in **1** and **2**, but are fewer in the presence of the carbonate. There are also multiple K–O contacts between the carbonate O atoms and the K⁺ cations in the tetramer, in which the distances for K1–O1 and K1–O3 are 2.656(2) and 2.656(3) Å, respectively, and K1–O2 is longer at 2.981(2) Å. One of the DME groups is disordered between two K⁺ cations. Bond valence analysis for the {O₆F₂} coordination sphere of K1 indicated a total of 1.18 for the K...F and K–O contributions, 15% of which is due to K...F interactions. The {O₆F₂} coordination of K2 resulted in a sum of 1.24 for bond valence, with 14% contributed by K...F contacts. The bond lengths for the K...F and K–O contacts are listed in Table S4

in the Supporting Information, however, only the intramolecular K...F and K–O contacts in one asymmetric unit of **8** are depicted in Figure 9 for clarity. The range of K...F distances for K1 and K2 is 2.818(3)–3.034(3) Å, similar to the distances found for complexes **1** and **2**.

The solution-based conductivity for **8** demonstrates weak electrolyte behavior in solution. The Onsager plot of **8** is shown along with solution conductivity studies of a dianionic [Cu(OAr^F)₄]²⁻ species^[20] in Figure S12 in the Supporting Information. The conductivity of **8** is very low in THF compared with similar concentrations of dianionic [Cu(OAr^F)₄]²⁻. The aforementioned K...F and K–O interactions are proposed to be maintained in solution, consistent with the tetramer observed in the solid state.

The Evans method^[32] magnetic moment of **8** was determined to be 3.00 μ_B in THF and 3.08 μ_B in acetone. The spin-only magnetic moment of 4.89 μ_B for an S=2 complex indicates that the four Cu^{II} centers are antiferromagnetically coupled, resulting in μ_{eff}=0.76 μ_B per Cu^{II} center. The lower solution μ_{eff} value again supports retention of the tetrameric structure in solution. In this compound, the carbonate group is the primary reason for a polynuclear structure, as is well-known in other multinuclear carbonate compounds.^[33]

Conclusion

The present K[Cu(OR)₂] complexes with fully (**1**, R=C₄F₉) or partially (**2**, R=CPhMe^F₂ or **3**, R=CMeMe^F₂) fluorinated alkoxides react rapidly with O₂ at –80 °C to form {Cu_n–O₂} species. The Cu/O₂ ratio of the oxygenated species is strongly affected by K...F/O interactions that keep Cu centers aggregated in solution. A higher degree of ligand fluorination in **1** favors the formation of the {Cu₃–O₂} adduct independent of Cu concentration due to extensive K...F/O interactions.

Complex **2** is one of the rare examples that can preferentially form tri- or binuclear Cu–O₂ adducts, depending on the Cu concentration. The {Cu₃–O₂} moiety forms as the dominant species from **2** and O₂ with [Cu^I] greater than 3 mM, whereas a 2:1 Cu/O₂ ratio for [Cu^I] less than 2 mM was observed. To the best of our knowledge, compound **3** is the first example of a Cu^I complex that can produce Cu–O₂ adducts with different Cu/O₂ stoichiometries controlled by not only [Cu^I] but also the O₂ diffusion rate. Slow O₂ diffusion into solutions of **3** with [Cu^I] greater than 3 mM generated a {Cu₃–O₂} species, whereas quickly saturating the solution with O₂ produces a dinuclear {Cu₂–O₂} complex independent of Cu concentration. Reduction of O₂ is irreversible for all complexes and concentrations studied. With C–H bonds present in the ligands, intramolecular hydroxylation of sp²- (**2**) and sp³-hybridized (**3**) C–H bonds is observed. Nucleophilic reactivity with CO₂ has also been shown and a Cu^{II} carbonate species has been isolated and characterized. Thus, these fluorinated alkoxides support {Cu_n–O₂} moieties with both electro- and nucleophilic character. Previously, alkali cations have been reported to increase the reactivity

of reduced mononuclear transition-metal complexes with CO^[34] and CO₂.^[35] More recently, Ca²⁺ has been shown to accelerate the rate of O₂ reduction in a Mn system^[36] and K⁺ has been shown to facilitate N₂ reduction by low-valent Fe.^[37] Thus, the pairing of d- and s-block metals for small-molecule activation may prove increasingly general. In biological systems, dioxygen reactivity of multinuclear Cu is mediated by intricate scaffolding of proteins with kilodalton molecular weights. Analogous multinuclear Cu chemistry has now been achieved with exclusively O-donor coordination, without bridging bulky ligands, and simply the 0.039 kDa K⁺ cation.

Experimental Section

General procedures: Ligand synthesis and Cu^I complex preparations were performed at RT in an MBraun purified N₂-filled drybox or by using standard Schlenk techniques under an atmosphere of N₂ or Ar. The anhydrous solvents CH₂Cl₂, diethyl ether, toluene, and hexanes were purified with an Ar-filled MBraun solvent purification system (SPS) equipped with dual columns of anhydrous Al₂O₃. Anhydrous THF (99.9%) was distilled under N₂ from purple sodium benzophenone ketyl and degassed before further treatment with calcium hydride in the drybox. Deuterated solvents used for NMR samples (CDCl₃ and CD₂Cl₂) and the internal ¹⁹F standard, trichlorofluoromethane (CFCl₃), were dried by heating at reflux over CaH₂; [D₆]acetone was dried over molecular sieves. All solvents were stored over molecular sieves in an N₂-filled drybox. Celite was dried overnight in vacuo while being heated to 125°C with an oil bath. The reagent 18C6 was obtained from commercial sources and recrystallized from hexanes. KH was obtained as a mineral oil dispersion (30 wt%) and purified by washing with hexanes and drying in vacuo prior to storage in the drybox. The fluorinated alcohols HOC₄F₉, HOC-(C₆H₅)(CF₃)₂, and HOC(CH₃)(CF₃)₂ were obtained from Oakwood Chemicals or Matrix Scientific and dried over sieves before being stored in the drybox. The perfluorinated *tert*-butoxide ligand, KOC₄F₉, was synthesized according to our reported modified procedure.^[10a] TBAPF₆ was triply recrystallized from CH₂Cl₂ and hexanes. [Cu(mes)]_n was synthesized by following a literature procedure.^[38] All other reagents were obtained from commercial sources and used without any further purification.

Physical methods: NMR spectra were recorded on Varian 300, 400, and 500 MHz spectrometers at RT. Chemical shifts (δ) for ¹H and ¹³C{¹H} NMR spectra were referenced to the resonance of residual protiosolvent (¹H) or the ¹³C{¹H} resonance of the solvent. Chemical shifts (δ) for ¹⁹F NMR spectra were referenced to internal CFCl₃. ³¹P{¹H} NMR spectra were collected with standard PPh₃ contained in a capillary tube within the NMR tube. Conductivity studies were performed at RT in the drybox by using a Fisher Scientific Traceable Portable Conductivity Meter (model number 09-326-2). Solutions for conductivity were prepared in CH₂Cl₂ or THF, depending on compound solubility. Triply recrystallized TBAPF₆ was used as the reference 1:1 electrolyte. ESI mass spectra were recorded by using an Agilent 1100 LC/MSD spectrometer equipped with mobile phases of water and MeCN with 0.1% formic acid. Elemental analyses were performed by Quantitative Technologies, Inc. (Whitehouse, NJ) or by Atlantic Microlab Inc. (Norcross, GA).

X-ray crystallography and structure determination: Single-crystal X-ray diffraction data were collected on a APEX-CCD detector equipped Bruker diffractometers. All Cu^I complexes structurally characterized were colorless crystals mounted on a Cryoloop with Paratone-N oil and cooled under a stream of nitrogen gas. Data were corrected for absorption by using semi-empirical, multiscan methods. All structures were solved by heavy-atom methods and the remaining non-hydrogen atoms were located from subsequent difference maps. Data were integrated by using the Bruker SHELXTL software program and scaled by using the

SADABS software program. Solution was by direct methods (SHELXS) and all non-hydrogen atoms were refined anisotropically by full-matrix least-squares methods (SHELXL-97). Hydrogen atoms were treated as idealized contributions and were placed in calculated positions with appropriate riding models for KOCMeMe^F₂. CHECKCIF indicated the presence of a large void volume (50 Å³), yet no appreciable residual electron density was found; use of PLATON Squeeze resulted in an electron count of 27 e⁻. In Ti(OC₄F₉), C3 was refined with an EADP command referenced to atom C1 and a large second weight correction factor was noted and kept with the refinement. Residual electron density greater than 1 e⁻ was noted near atoms F9 (1.58 e⁻ at 1.25 Å), F6 (1.41 e⁻ at 1.13 Å), and F3 (1.35 e⁻ at 1.08 Å) in Ti(OC₄F₉). There were some minor distortions with respect to some of the fluorine atoms in complex **1**, but these were not treated. The X-ray structure was twinned for **4** and solved by using appropriate corrections, however, the statistics were still poor. All non-hydrogen atoms were refined anisotropically by Fourier full-matrix least squares on *F*² and hydrogen atoms were placed in calculated positions with appropriate riding models for compound **6**. For compound **8**, disordered atoms in DME molecules were at 50% occupancy. All software is contained in various libraries (SHELXTL, SMART, and SAINT) maintained by Bruker AXS, Madison, WI,^[39] except CHECKCIF, which is a service of the International Union of Crystallography.

CCDC-899244-899252 contain the supplementary crystallographic data for this paper. These data can be obtained free of charge from The Cambridge Crystallographic Data Centre via www.ccdc.cam.ac.uk/data_request/cif.

Low-temperature UV/Vis spectroscopy and generation of {Cu₂O₂} species: Under a nitrogen atmosphere within a glove box, K[Cu(OR)₂] complexes (**1–3**) were dissolved in O₂-free THF (3 mL), giving a range of colors to pale-yellow solutions, depending on the compound. The cuvette with a side arm was sealed with a septum covered by parafilm, quickly removed from the glove box, and cooled to 193 K in a Shimadzu UV-3600 spectrophotometer equipped with a Unisoku thermostated cell holder. O₂ from a RT balloon (99.999%) was gently bubbled through the reaction solution. After full formation of {Cu₂O₂} species, excess O₂ was removed by purging ultrapure Ar gas through the headspace for about 2–3 min.

Ligand syntheses

KOCPhMe^F₂: A slurry of KH (0.2750 g, 6.856 mmol) in Et₂O was cooled to -78°C by using a dry ice/acetone bath. A deficiency of HOCPhMe^F₂ (1.510 g, 6.185 mmol) was syringed into the solution slowly, while the flask was flushed with N₂. The reaction mixture was cloudy white and kept cold for approximately 2 h before being warmed to RT over 4 h. The solvent was removed in vacuo to yield white solid residue coating the flask, which was brought into an N₂-filled drybox. The white solid was redissolved in Et₂O and filtered over Celite to remove excess KH, and the filtrate was dried under vacuum, yielding a white powder. The crude solid was dissolved in 1:1 Et₂O/hexanes and layered with hexanes for recrystallization (-34°C). After two recrystallizations, a white solid was obtained (88%, 1.537 g). Colorless block crystals suitable for single-crystal X-ray diffraction were isolated from the same recrystallization conditions. ¹H NMR (300 MHz, (CD₃)₂CO): δ = 7.88 (m, 1H; OC(*p*-C₆H₅)(CF₃)₂), 7.37 ppm (m, 4H; OC(*o*- and *m*-C₆H₅)(CF₃)₂); ¹³C NMR (75 MHz, (CD₃)₂CO): δ = 144.1 (s, OC(*ipso*-C₆H₅)(CF₃)₂), 129.0 (s, OC(*m*-C₆H₅)(CF₃)₂), 128.6 (s, OC(*p*-C₆H₅)(CF₃)₂), 128.3 (s, OC(*o*-C₆H₅)(CF₃)₂), 127.9 (quartet, OC(C₆H₅)(CF₃)₂), ¹J(C,F) = 293.5 Hz), 83.7 ppm (septet, OC(C₆H₅)(CF₃)₂), ²J(C,F) = 25.2 Hz); ¹⁹F NMR (282 MHz, (CD₃)₂CO): δ = -75.45 ppm (s, OCPH(CF₃)₂); elemental analysis calcd (%) for C₉H₅OF₆K: C 38.30, H 1.79, F 40.39; found: C 38.37, H 2.03, F 40.30.

KOCMeMe^F₂: A slurry of KH (1.6882 g, 42.09 mmol) in Et₂O was cooled to -78°C by using a dry ice/acetone bath. A deficiency of HOCMeMe^F₂ (6.826 g, 37.49 mmol) was syringed into the solution slowly, while the flask was flushed with N₂. The stirred reaction mixture was cloudy white and kept cold for approximately 2 h before being warmed to RT over 4 h. The solvent was removed in vacuo to yield off-white solid coating the flask, which was brought into an N₂-filled drybox. The solid residue was redissolved in Et₂O and filtered over Celite to remove excess KH and

the filtrate was dried under vacuum, yielding an off-white powder. The crude solid was dissolved in 1:1 Et₂O/hexanes and layered with hexanes for recrystallization (−34°C). After two recrystallizations, a white solid was obtained (67%, 5.5417 g). Colorless block crystals suitable for single-crystal X-ray diffraction were isolated from the same recrystallization conditions. (Fluorine analysis was likely to be low due to incomplete F combustion.) ¹H NMR (400 MHz, (CD₃)₂CO): δ = 1.27 ppm (s, OC(CH₃)(CF₃)₂); ¹³C NMR (100 MHz, (CD₃)₂CO): δ = 128.2 (quartet, OC(CH₃)(CF₃)₂), ¹J(C,F) = 293.4 Hz, 79.2 (septet, OC(CH₃)(CF₃)₂), ²J(C,F) = 25.3 Hz, 21.5 ppm (OC(CH₃)(CF₃)₂); ¹⁹F NMR (376 MHz, (CD₃)₂CO): δ = −79.58 ppm (s, OC(CH₃)(CF₃)₂); elemental analysis calcd (%) for C₄H₃OF₆K: C 21.82, H 1.37, F 51.78; found: C 21.64, H 1.65, F 50.00.

Tl(OC₄F₉): A solution of HOC₄F₉ (4.91 g, 20.80 mmol) in CH₂Cl₂ was cooled to −78°C by using a dry ice/acetone bath and flushed with N₂. Thallium ethoxide (5.0 g, 20.04 mmol) was slowly syringed into the solution. A white precipitate formed upon mixing and the solution was very pale purple. The reaction was kept cold for approximately 1 h before being warmed to RT over 2 h. Stirring was stopped and the white precipitate was allowed to settle to the bottom of the flask, after which time the solution layer was removed by using a cannula. The white solid was washed three times with a total of 30 mL of anhydrous CH₂Cl₂, and the solid was dried in vacuo and brought into the N₂-filled drybox. The crude white solid was redissolved in toluene/THF, filtered to remove any insoluble particulate, yielding a very pale purple solution. The product was recrystallized by layering the solution in toluene/THF with hexanes and stored at −34°C. After two recrystallizations, white solid was obtained (71%, 6.2822 g) and colorless crystal blocks suitable for single-crystal X-ray diffraction were isolated from the same recrystallization mixture. ¹³C NMR (75 MHz, (CD₃)₂CO): δ = 125.5 (quartet, OC(CF₃)₃), ¹J(C,F) = 296.6 Hz, 83.5 ppm (decet, OC(CF₃)₃), ²J(C,F) = 28.4 Hz; ¹⁹F NMR (282 MHz, (CD₃)₂CO): δ = −74.02 ppm (s, OC(CF₃)₃); elemental analysis calcd (%) for C₄F₉O₂Tl: C 10.93, F 38.91; found: C 10.87, F 38.87.

Copper(I) alkoxide complex syntheses

K[Cu(OC₄F₉)₂] (1): A portion of HOC₄F₉ (0.3284 g, 1.39 mmol) was syringed into a yellow slurry of [Cu(mes)]_n (0.2530 g, 1.39 mmol) in Et₂O. The reaction mixture was yellow and slightly cloudy. A colorless solution of KOC₄F₉ (0.3811 g, 1.39 mmol) in Et₂O was added and the mixture stirred for 2 h at RT. The cloudy yellow solution was filtered over Celite to remove any insoluble material, and the bright yellow filtrate was concentrated to dryness in vacuo. The resultant yellow solid residue was washed twice with hexanes to remove mesitylene (Hmes), then the solid was dried in vacuo, yielding a pale yellow powder, and recrystallized by using Et₂O/hexanes to obtain a microcrystalline solid (62%, 0.4935 g). If drybox conditions were not optimal, recrystallization attempts resulted in an orange insoluble material precipitating from solution; this significantly lowered the yield, making the pure yellow solid difficult to recover. Colorless crystals suitable for single-crystal X-ray diffraction were grown slowly from the same Et₂O/hexanes recrystallization mixture at −34°C. Satisfactory elemental analyses could not be obtained due to the exceptional sensitivity of **1** to O₂ and the high degree of fluorination. ¹³C NMR (125 MHz, (CD₃)₂CO): δ = 123.9 (q, C(CF₃)₃), ¹J(C,F) = 293.4 Hz, 84.1 ppm (decet, C(CF₃)₃), ²J(C,F) = 27.7 Hz; ¹⁹F NMR (470 MHz, (CD₃)₂CO): δ = −75.35 ppm (s, OC(CF₃)₃); ESI-MS (CH₂Cl₂) negative scan: *m/z*: 235 [−OC₄F₉], 533/535 [Cu(OC₄F₉)₂][−]; positive scan: *m/z*: 145/147 [Cu(MeCN)₂]⁺.

K[Cu(OCPhMe^F)₂] (2): A portion of HOCPhMe^F (0.3366 g, 1.38 mmol) was added to a yellow slurry of [Cu(mes)]_n (0.2517 g, 1.38 mmol) in Et₂O. The reaction mixture was yellow and slightly cloudy. A solution of KOCPhMe^F (0.3901 g, 1.38 mmol) in Et₂O was added and the mixture stirred for 2 h at RT. Complex **2** was obtained by using a workup analogous to that of **1**. The pale yellow solid was recrystallized from a mixture of Et₂O and hexanes (84%, 0.6835 g). Pale yellow crystals suitable for single-crystal X-ray diffraction were grown from the same mixture at −34°C. ¹H NMR (500 MHz, (CD₃)₂CO): δ = 7.94 (m, 1H; OC(*p*-C₆H₃)(CF₃)₂), 7.29 ppm (m, 4H; OC(*o*- and *m*-C₆H₃)(CF₃)₂); ¹³C NMR (125 MHz, (CD₃)₂CO): δ = 139.4 (s, OC(*ipso*-C₆H₃)(CF₃)₂), 129.1 (s, OC(*m*-C₆H₃)(CF₃)₂), 128.4 (s, OC(*p*-C₆H₃)(CF₃)₂), 128.2 (s, OC(*o*-C₆H₃)(CF₃)₂), 126.3 (quartet, OC(C₆H₃)(CF₃)₂), ¹J(C,F) = 291.1 Hz, 82.4 ppm

(septet, OC(C₆H₃)(CF₃)₂), ²J(C,F) = 26.5 Hz; ¹⁹F NMR (470 MHz, (CD₃)₂CO): δ = −74.56 ppm (s, OCPh(CF₃)₂); elemental analysis calcd (%) for C₁₈H₁₀O₂F₁₂KCu: C 36.71, H 1.71, F 38.71; found: C 36.45, H 1.46, F 38.86.

K[Cu(OCMeMe^F)₂] (3): A portion of HOCMeMe^F (0.25233 g, 1.39 mmol) was added to a yellow slurry of [Cu(mes)]_n (0.2519 g, 1.38 mmol) in Et₂O. The reaction mixture was yellow and slightly cloudy. A solution of KOCMeMe^F (0.3060 g, 1.39 mmol) in Et₂O was added and the mixture was stirred for 2 h at RT. Complex **3** was obtained by using a workup analogous to that of **1**. The yellow solid was recrystallized by using Et₂O/hexanes and a microcrystalline solid was obtained (71%, 0.4561 g). ¹H NMR (500 MHz, (CD₃)₂CO): δ = 1.40 ppm (s, OC(CH₃)(CF₃)₂); ¹³C NMR (125 MHz, (CD₃)₂CO): δ = 126.8 (q, OC(CH₃)(CF₃)₂), ¹J(C,F) = 279.6 Hz, 78.5 (septet, OC(CH₃)(CF₃)₂), ²J(C,F) = 23.03 Hz, 23.1 ppm (s, OC(CH₃)(CF₃)₂); ¹⁹F NMR (470 MHz, (CD₃)₂CO): δ = −78.5 ppm (s, OC(CH₃)(CF₃)₂); elemental analysis calcd (%) for C₈H₆O₂F₁₂KCu: C 20.67, H 1.30, F 49.05; found: C 20.78, H 1.21, F 48.85.

[K(18C6)][Cu(OC₄F₉)₂] (4): A solution of 18C6 (0.2163 g, 0.818 mmol) in toluene (10 mL) was added to a slurry of **1** (0.4689 g, 0.819 mmol) in toluene (10 mL). The immediately cloudy yellow solution was left stirring at RT overnight. The resulting cloudy, pale yellow solution was filtered to remove any yellow insoluble precipitate and the clear, colorless filtrate was concentrated to dryness in vacuo. The white solid was soluble in CH₂Cl₂ and recrystallized from layering a solution in CH₂Cl₂ with hexanes (72%, 0.4940 g). Colorless crystals suitable for single-crystal X-ray diffraction were grown from the same recrystallization conditions at −34°C. ¹H NMR (500 MHz, CD₂Cl₂): δ = 3.62 ppm (s, C₁₂O₆H₂₄); ¹³C NMR (125 MHz, CD₂Cl₂): δ = 123.3 (quartet, OC(CF₃)₃), ¹J(C,F) = 294.9 Hz, 83.5 (decet, OC(CF₃)₃), ²J(C,F) = 27.7 Hz, 70.7 ppm (s, C₁₂O₆H₂₄); ¹⁹F NMR (470 MHz, CD₂Cl₂): δ = −75.99 ppm (s, OC₄F₉); ESI-MS (CH₂Cl₂) negative scan: *m/z*: 235 [−OC₄F₉], 533/535 [Cu(OC₄F₉)₂][−]; positive scan: *m/z*: 145/147 [Cu(MeCN)₂]⁺, 303 [K18C6]⁺; elemental analysis calcd (%) for C₂₀H₂₄O₈F₁₈KCu: C 28.70, H 2.89, F 40.86; found: C 28.70, H 2.49, F 40.47.

[K(18C6)][Cu(OCPhMe^F)₂] (5): A solution of 18C6 (0.2477 g, 0.937 mmol) in toluene (10 mL) was added to a slurry of **2** (0.6375 g, 1.083 mmol) in toluene (10 mL). After a workup analogous to **4**, complex **5** was obtained as a white solid. Recrystallized solid was obtained in 72% yield (0.5733 g). ¹H NMR (500 MHz, CD₂Cl₂): δ = 7.90 (m, 1H; OC(*p*-C₆H₃)(CF₃)₂), 7.29 (m, 4H; OC(*o*- and *m*-C₆H₃)(CF₃)₂), 3.68 ppm (s, 24H; C₁₂H₂₄O₆); ¹³C NMR (125 MHz, CD₂Cl₂): δ = 139.2 (s, OC(*ipso*-C₆H₃)(CF₃)₂), 128.8 (s, OC(*m*-C₆H₃)(CF₃)₂), 128.1 (s, OC(*p*-C₆H₃)(CF₃)₂), 127.9 (s, OC(*o*-C₆H₃)(CF₃)₂), 126.0 (quartet, OC(C₆H₃)(CF₃)₂), ¹J(C,F) = 291.9 Hz, 82.2 (septet, OC(C₆H₃)(CF₃)₂), ²J(C,F) = 26.5 Hz, 70.7 ppm (s, C₁₂H₂₄O₆); ¹⁹F NMR (470 MHz, CD₂Cl₂): δ = −75.27 ppm (s, OC(C₆H₃)(CF₃)₂); ESI-MS (CH₂Cl₂) negative scan: *m/z*: 243 [−OCPhMe^F]; positive scan: *m/z*: 145/147 [Cu(MeCN)₂]⁺, 303 [K18C6]⁺; elemental analysis calcd (%) for C₃₀H₃₄O₈F₁₂KCu: C 42.23, H 4.02, F 26.72; found: C 42.30, H 3.65, F 26.72.

[K(18C6)][Cu(OCMeMe^F)₂] (6): A solution of 18C6 (0.1914 g, 0.724 mmol) in toluene (10 mL) was added to a slurry of **3** (0.3352 g, 0.721 mmol) in toluene (10 mL). After a workup analogous to **4**, complex **6** was obtained as a white solid. The solid was recrystallized from a concentrated solution in toluene and layered with hexanes (69%, 0.3634 g). Colorless crystals suitable for X-ray analysis were grown from the same recrystallization conditions at −34°C. ¹H NMR (500 MHz, CD₂Cl₂): δ = 3.62 (s, 24H; C₁₂O₆H₂₄), 1.44 ppm (s, 3H; OC(CH₃)(CF₃)₂); ¹³C NMR (125 MHz, CD₂Cl₂): δ = 126.6 (quartet, OC(CH₃)(CF₃)₂), ¹J(C,F) = 291.0 Hz, 78.4 (septet, OC(CH₃)(CF₃)₂), ²J(C,F) = 26.4 Hz, 70.7 (s, C₁₂H₂₄O₆), 23.7 ppm (s, OC(CH₃)(CF₃)₂); ¹⁹F NMR (470 MHz, CD₂Cl₂): δ = −79.22 ppm (s, OC(CH₃)(CF₃)₂); ESI-MS (CH₂Cl₂) positive scan: *m/z*: 145/147 [Cu(MeCN)₂]⁺, 303 [K18C6]⁺; elemental analysis calcd (%) for C₂₀H₃₀O₈F₁₂KCu: C 32.95, H 4.15, F 31.27; found: C 33.17, H 4.07, F 30.73.

(Ph₃P)[Cu(OC₄F₉)₂] (7): A portion of HOC₄F₉ (0.0576 g, 0.2439 mmol) was added to a yellow slurry of [Cu(mes)]_n (0.0423 g, 0.2315 mmol) in Et₂O. After being stirred for 5 min, the reaction mixture was yellow and slightly cloudy. A solution of Tl(OC₄F₉) (0.1010 g, 0.2298 mmol) in THF

was added to the mixture and stirred for 2 h at RT. A portion of Ph_4PI (0.1082 g, 0.2320 mmol) was added by using Et_2O and bright yellow precipitate (presumably TII) formed immediately. The cloudy yellow mixture was stirred for 2 h and filtered over Celite to remove any insoluble TII. The filtrate was very pale yellow and the solvent was removed in vacuo. The resultant off-white residue was washed and triturated twice with hexanes and CH_2Cl_2 , respectively, to remove Hmes. The product was obtained as a white solid (79%, 0.1588 g) after recrystallization from $\text{CH}_2\text{Cl}_2/\text{hexanes}$. Colorless needles suitable for single-crystal X-ray diffraction studies were grown very slowly from CH_2Cl_2 and hexanes at -34°C . $^1\text{H NMR}$ (400 MHz, CD_2Cl_2): $\delta=7.93$ (t, 4H; (*p*- C_6H_5) $_4\text{P}$), 7.78 (m, 8H; (*m*- C_6H_5) $_4\text{P}$), 7.63 ppm (m, 8H; (*o*- C_6H_5) $_4\text{P}$); $^{13}\text{C NMR}$ (100 MHz, CD_2Cl_2): $\delta=135.9$ (s, 1C, (*p*- C_6H_5) $_4\text{P}$), 134.5 (s, (*o*- C_6H_5) $_4\text{P}$), 131.2 (s, (*m*- C_6H_5) $_4\text{P}$), 123.4 (quartet, $\text{OC}(\text{CF}_3)_3$, $^1J(\text{C},\text{F})=294.9$ Hz), 118.4 (s, (*ipso*- C_6H_5) $_4\text{P}$), 83.4 ppm (decet, $\text{OC}(\text{CF}_3)_3$, $^2J(\text{C},\text{F})=27.8$ Hz); $^{19}\text{F NMR}$ (376 MHz, CD_2Cl_2): $\delta=-75.47$ ppm (s, $\text{OC}(\text{CF}_3)_3$); ESI-MS (CH_2Cl_2) negative scan: m/z : 235 [$-\text{OC}_4\text{F}_9$], 533/535 [$\text{Cu}(\text{OC}_4\text{F}_9)_2$] $^-$; positive scan: m/z : 145/147 [$\text{Cu}(\text{MeCN})_2$] $^+$, 339 [Ph_4P] $^+$; elemental analysis calcd (%) for $\text{C}_{32}\text{H}_{20}\text{O}_2\text{F}_{18}\text{PCu}$: C 44.03, H 2.31, F 39.17; found: C 40.2(7), H 2.0(2) (the CH analyses represents an average of six replicate runs), F 39.12.

Cu^{II} carbonate complex synthesis

($[\text{K}_2(\text{DME})_{1.5}][\text{Cu}(\text{OCMeMe}^{\text{F}})_2(\text{CO}_3)]_4$) (8): A solution of **3** (0.2905 g, 0.625 mmol) was prepared in THF (40 mL). The pale yellow solution was placed in a Schlenk flask, flushed with N_2 , and cooled to -78°C . After equilibrating at -78°C for 10 min under N_2 , O_2 was introduced by directly bubbling the gas into the Cu^{I} solution. The color immediately changed to deep brown and the reaction with O_2 continued for 30 min. While maintaining the temperature at -78°C , excess O_2 was removed from the headspace by purging with N_2 , and CO_2 was then bubbled into the brown solution for 20 min. When the solution was warmed to RT, there was a distinct color change to deep emerald green. The solvent was removed under vacuum and a green powdery residue remained in the flask, which was brought back into a N_2 -filled drybox for workup and recrystallization. The solid was redissolved in THF (5 mL) and the dark green solution was filtered to remove some dark, insoluble precipitate. The solution was layered with hexanes (15 mL) and placed in the freezer for recrystallization. Further recrystallization with DME and hexanes resulted in the growth of blue crystals suitable for single-crystal X-ray diffraction studies. The blue single-crystalline solid was obtained in 35% yield, based on the $[\text{Cu}_2\text{O}_2]$ stoichiometry (0.0533 g) and was separated from a dark green sticky material that co-precipitated from green DME/hexanes solution. UV/Vis (DME): $\lambda_{\text{max}}=280$ ($\epsilon=3958$), 668 nm ($57\text{ cm}^{-1}\text{M}^{-1}$); IR (neat): $\tilde{\nu}=2963$ ($\nu\text{C-H}$), 1552 (νCO_3), 1459 (νCO_3), 1300, 1199 ($\nu\text{C-F}$), 1175, 957 ($\nu\text{Cu-OR}$), 700 cm^{-1} ($\nu\text{C-F}$ and $\nu\text{Cu-OR}$); elemental analysis calcd (%) for $\text{K}_2\text{C}_{15}\text{H}_{21}\text{O}_8\text{F}_{12}\text{Cu}$: C 25.77, H 3.03, F 32.61; found: C 25.55, H 2.81, F 32.64; μ_{eff} (Evans method, $[\text{D}_8]\text{THF}$) = 3.00 μ_{B} ; μ_{eff} (Evans method, $[\text{D}_6]\text{acetone}$) = 3.08 μ_{B} .

Acknowledgements

We are grateful for the financial support of Boston University, the National Science Foundation (CHE 0910647 and CHE 0619339) and the ACS Petroleum Research Fund (48022-AC3). We thank Professor J. P. Caradonna and Dr. P. C. Tarves for helpful advice and sharing facilities and Professors Steven H. Strauss and William B. Tolman for thoughtful discussions.

- [1] a) Z. T. r. K. D. Karlin, *Bioinorganic Chemistry of Copper*, Chapman & Hall: New York, **1993**, pp; b) N. Kitajima, Y. Moro-oka, *Chem. Rev.* **1994**, *94*, 737–757; c) A. D. Z. K. D. Karlin, *Bioinorganic Catalysis*, Marcel Dekker, New York, **1999**, pp; d) W. B. Tolman, A. G. Blackman, *Struct. Bonding* **2000**, *97*, 179–211.
[2] a) U. M. S. E. I. Solomon, T. E. Machonkin, *Chem. Rev.* **1996**, *96*, 2563–2605; b) P. C. E. I. Solomon, M. Metz, S.-K. Lee, A. E.

- Palmer, *Angew. Chem.* **2001**, *113*, 4702–4724; *Angew. Chem. Int. Ed.* **2001**, *40*, 4570–4590; c) J.-L. P. M. Fontecave, *Coord. Chem. Rev.* **1998**, *170*, 125–140.
[3] a) L. M. Mirica, X. Ottenwaelder, T. D. P. Stack, *Chem. Rev.* **2004**, *104*, 1013–1046; b) K. D. Karlin, Y. Gultneh, *Prog. Inorg. Chem.* **1987**, *35*, 219–327; c) E. A. Lewis, W. B. Tolman, *Chem. Rev.* **2004**, *104*, 1047–1076.
[4] B. Borup, W. E. Streib, K. G. Caulton, *Inorg. Chem.* **1997**, *36*, 5058–5063.
[5] A. P. Purdy, C. F. George, *Inorg. Chem.* **1991**, *30*, 1969–1970.
[6] A. H. G. Santiso-Quinones, J. Schaefer, R. Brückner, C. Knapp, I. Krossing, *Chem. Eur. J.* **2009**, *15*, 6663.
[7] K. G. Caulton, L. G. Hubert-Pfalzgraf, *Chem. Rev.* **1990**, *90*, 969–995.
[8] A. P. Purdy, C. F. George, G. A. Brewer, *Inorg. Chem.* **1992**, *31*, 2633–2638.
[9] A. P. Purdy, C. F. George, *Polyhedron* **1998**, *17*, 4041–4048.
[10] a) S. A. Cantalupo, J. S. Lum, M. C. Buzzeo, C. Moore, A. G. DiPasquale, A. L. Rheingold, L. H. Doerrer, *Dalton Trans.* **2010**, *39*, 374–383; b) S. A. Cantalupo, H. E. Ferreira, E. Bataineh, A. J. King, M. V. Petersen, T. Wojtasiewicz, A. G. DiPasquale, A. L. Rheingold, L. H. Doerrer, *Inorg. Chem.* **2011**, *50*, 6584–6596.
[11] M. C. Buzzeo, A. H. Iqbal, C. M. Long, D. Millar, S. Patel, M. A. Pellow, S. A. Saddoughi, A. L. Smenton, J. F. C. Turner, J. D. Wadhwani, R. G. Compton, J. A. Golen, A. L. Rheingold, L. H. Doerrer, *Inorg. Chem.* **2004**, *43*, 7709–7725.
[12] B. Zheng, M. O. Miranda, A. G. DiPasquale, J. A. Golen, A. L. Rheingold, L. H. Doerrer, *Inorg. Chem.* **2009**, *48*, 4274–4276.
[13] M. V. Childress, D. Millar, T. M. Alam, K. A. Kreisel, G. P. A. Yap, L. N. Zakharov, J. A. Golen, A. L. Rheingold, L. H. Doerrer, *Inorg. Chem.* **2006**, *45*, 3864–3877.
[14] M. Håkansson, C. Lopes, S. Jagner, *Inorg. Chim. Acta* **2000**, *304*, 178–183.
[15] A. Reisinger, N. Trapp, I. Krossing, *Organometallics* **2007**, *26*, 2096–2105.
[16] J. A. Samuels, K. Folting, J. C. Huffman, K. G. Caulton, *Chem. Mater.* **1995**, *7*, 929–935.
[17] A. P. G. Purdy, C. F. Callahan, *Inorg. Chem.* **1991**, *30*, 2812.
[18] P. K. Mehrotra, R. Hoffmann, *Inorg. Chem.* **1978**, *17*, 2187–2189.
[19] M. A. Carvajal, S. Alvarez, J. J. Novoa, *Chem. Eur. J.* **2004**, *10*, 2117–2132.
[20] I. D. Brown, D. Altermatt, *Acta Crystallogr. Sect. B* **1985**, *41*, 244–247.
[21] N. E. Brese, M. O’Keeffe, *Acta Crystallogr. Sect. B* **1991**, *47*, 192–197.
[22] a) R. D. Feltham, R. G. Hayter, *J. Chem. Soc.* **1964**, 4587–4591; b) W. J. Geary, *Coord. Chem. Rev.* **1971**, *7*, 81–122.
[23] C. J. Willis, *Coord. Chem. Rev.* **1988**, *88*, 133–202.
[24] S. F. Hannigan, J. S. Lum, J. W. Bacon, J. A. Golen, A. L. Rheingold, L. H. Doerrer, *Organometallics* **2013**, accepted.
[25] H. F. A.-K. C. A. McAuliffe, D. S. Barratt, J. C. Briggs, A. Challita, A. Hosseini, M. G. Little, A. G. Mackie, K. Minten, *J. Chem. Soc. Dalton Trans.* **1983**, 2147–2153.
[26] a) K. D. K. Z. Tyeklar, *Acc. Chem. Res.* **1989**, *22*, 241–248; b) M. Suzuki, *Acc. Chem. Res.* **2007**, *40*, 609–617.
[27] a) A. P. Cole, D. E. Root, P. Mukherjee, E. I. Solomon, T. D. P. Stack, *Science* **1996**, *273*, 1848–1850; b) P. Kang, E. Bobyr, J. Dustman, K. O. Hodgson, B. Hedman, E. I. Solomon, T. D. P. Stack, *Inorg. Chem.* **2010**, *49*, 11030–11038; c) M. Taki, S. Teramae, S. Nagatomo, Y. Tachi, T. Kitagawa, S. Itoh, S. Fukuzumi, *J. Am. Chem. Soc.* **2002**, *124*, 6367–6377; d) A. K. Gupta, W. B. Tolman, *Inorg. Chem.* **2012**, *51*, 1881–1888.
[28] a) I. Sanyal, R. W. Strange, N. J. Blackburn, K. D. Karlin, *J. Am. Chem. Soc.* **1991**, *113*, 4692–4693; b) G. Kolks, S. J. Lippard, J. V. Waszczak, *J. Am. Chem. Soc.* **1980**, *102*, 4832–4833.
[29] K. Nakamoto, *Infrared and Raman Spectra of Inorganic and Coordination Compounds*, Wiley, New York, **1978**, p. 448.
[30] SDBSWeb: <http://riodb01.ibase.aist.go.jp/sdbs/> (National Institute of Advanced Industrial Science and Technology, 23 July 2012).

- [31] L. Yang, D. R. Powell, R. P. Houser, *Dalton Trans.* **2007**, 955–964.
- [32] a) D. F. Evans, *J. Chem. Soc.* **1959**, 2003–2005; b) S. K. Sur, *J. Magn. Reson.* **1989**, *82*, 169–173.
- [33] D. A. Palmer, R. Van Eldik, *Chem. Rev.* **1983**, *83*, 651–731.
- [34] M. Y. Darensbourg, D. J. Darensbourg, D. Burns, D. A. Drew, *J. Am. Chem. Soc.* **1976**, *98*, 3127–3136.
- [35] a) S. Gambarotta, F. Arena, C. Floriani, P. F. Zanazzi, *J. Am. Chem. Soc.* **1982**, *104*, 5082–5092; b) J. S. Silvia, C. C. Cummins, *Chem. Sci.* **2011**, *2*, 1474–1479.
- [36] Y. J. Park, J. W. Ziller, A. S. Borovik, *J. Am. Chem. Soc.* **2011**, *133*, 9258–9261.
- [37] T. M. Figg, P. L. Holland, T. R. Cundari, *Inorg. Chem.* **2012**, *51*, 7546–7550.
- [38] T. Tsuda, T. Yazawa, K. Watanabe, T. Fujii, T. Saegusa, *J. Org. Chem.* **1981**, *46*, 192–194.
- [39] G. M. Sheldrick, *Acta Crystallogr. Sect. A* **2008**, *64*, 112–122.

Received: December 1, 2012
Published online: March 19, 2013